NANO LETTERS

pubs.acs.org/NanoLett

Large Scale Growth and Characterization of Atomic Hexagonal Boron Nitride Layers

Li Song,[†] Lijie Ci,[†] Hao Lu,[†] Pavel B. Sorokin,[†] Chuanhong Jin,[‡] Jie Ni,[†] Alexander G. Kvashnin,[§] Dmitry G. Kvashnin,[§] Jun Lou,[†] Boris, I. Yakobson,[†] and Pulickel M. Ajayan*,[†]

[†]Department of Mechanical Engineering & Materials Science, Rice University, Houston, Texas 77005, [‡]Nanotube Research Center, National Institute of Advanced Industrial Science and Technology (AIST), Tsukuba 305-8565, Japan, and [§]Siberian Federal University, 79 Svobodny av., Krasnoyarsk, 660041, Russia

ABSTRACT Hexagonal boron nitride (h-BN), a layered material similar to graphite, is a promising dielectric. Monolayer h-BN, so-called "white graphene", has been isolated from bulk BN and could be useful as a complementary two-dimensional dielectric substrate for graphene electronics. Here we report the large area synthesis of h-BN films consisting of two to five atomic layers, using chemical vapor deposition. These atomic films show a large optical energy band gap of 5.5 eV and are highly transparent over a broad wavelength range. The mechanical properties of the h-BN films, measured by nanoindentation, show 2D elastic modulus in the range of 200−500 N/m, which is corroborated by corresponding theoretical calculations.

KEYWORDS Boron nitride, electrical microscopy, optical and mechanical properties, computation

Boron nitride (BN) is a wide band gap III−V compound with remarkable physical properties and chemical stability. Hexagonal BN is comprised of alternating boron and nitrogen atoms in a honeycomb arrangement, consisting of sp^2-bonded two-dimensional (2D) layers.[1−5] Within each layer of hexagonal BN, boron and nitrogen atoms are bound by strong covalent bonds, whereas the layers are held together by weak van der Waals forces, as in graphite. Therefore, h-BN films could be peeled off from bulk BN crystal by micromechanical cleavage[4−6] and used as a dielectric layer.[6,7] Few-layer hexagonal BN has also been made by ultrasonication[8] and high-energy electron beam irradiation of BN particles.[9] The chemical decomposition reactions of various precursors have been used to demonstrate the growth of single layer BN domains over small areas.[10−13] However, methods for preparing good quality h-BN layers over large areas would bring new opportunities to exploit its properties and potential applications, especially as interesting two-dimensional dielectric material in graphene-based electronics. Here we show uniform and continuous h-BN films on a large area have been successfully synthesized using a thermal catalytic chemical vapor deposition (CVD) method. These as-grown films consisting of two to five layers are highly transparent with a large band gap and pose unique mechanical properties.

The synthesis of h-BN films was carried out in a split tube furnace with a fused quartz processing tube (50 mm outside diameter). A copper foil with 25 μm thickness was used as substrate, similar to previous reports.[14−16] For the growth, the Cu foil was quick washed by dilication nitric acid and deionized water. Then it was placed in the center of a furnace, annealed at 600 °C for 20 min in Ar/H_2 (15 vol % H_2, 85 vol % argon) flow with 500 sccm. As followed, the furnace was gradually heated up to 1000 °C in 40 min. Ammonia borane (NH_3−BH_3) was sublimated at 120−130 °C by using a heating belt and then carried into the reaction region by Ar/H_2 gas glow. During the growth process, Ar/H_2 flow was kept as 200 sccm. The typical growth time is 30−60 min. After growth, the furnace was cooled down to room temperature quickly. After growth, the films were coated with poly(methyl methacrylate) and transferred to other substrates for further characterization as reported previously in graphene transfers.[16,17] For characterization, JEOL-2100 field emission HRTEM was performed for high-resolution transmission electron microscopy (HRTEM), selected area electron diffraction (SAED), electron energy loss spectroscopy (EELS) measurements, and elemental mapping (Gatan GIF). JEOL-2010F, equipped with a postspecimen aberration corrector (CEOS), was carried out to obtain the atomic image. X-ray photoelecton spectroscopy (XPS) (PHI Quantera XPS) was performed using monochromatic aluminum Kα X-rays, and the MultiPak software was used for XPS data analyses. Raman spectroscopy (Renishaw inVia) was performed at 514.5 nm laser excitation. Electrical measurement was performed in a probe station with a high vacuum chamber. Optical absorption measurement (SHIMADZU UV-3600) was performed on h-BN films that were transferred onto optical quartz plates. For the mechanical tests, the as-grown h-BN film was transferred on a silicon wafer with around 1 μm well patterns. Atomic force micros-

* To whom correspondence should be addressed: tel, 1-713-3485904; fax, 1-713-3485423; e-mail, ajayan@rice.edu.

Received for review: 06/23/2010
Published on Web: 00/00/0000

DOI: 10.1021/nl1022139 | *Nano Lett.* **XXXX,** *xxx,* 000–000

NANO LETTERS

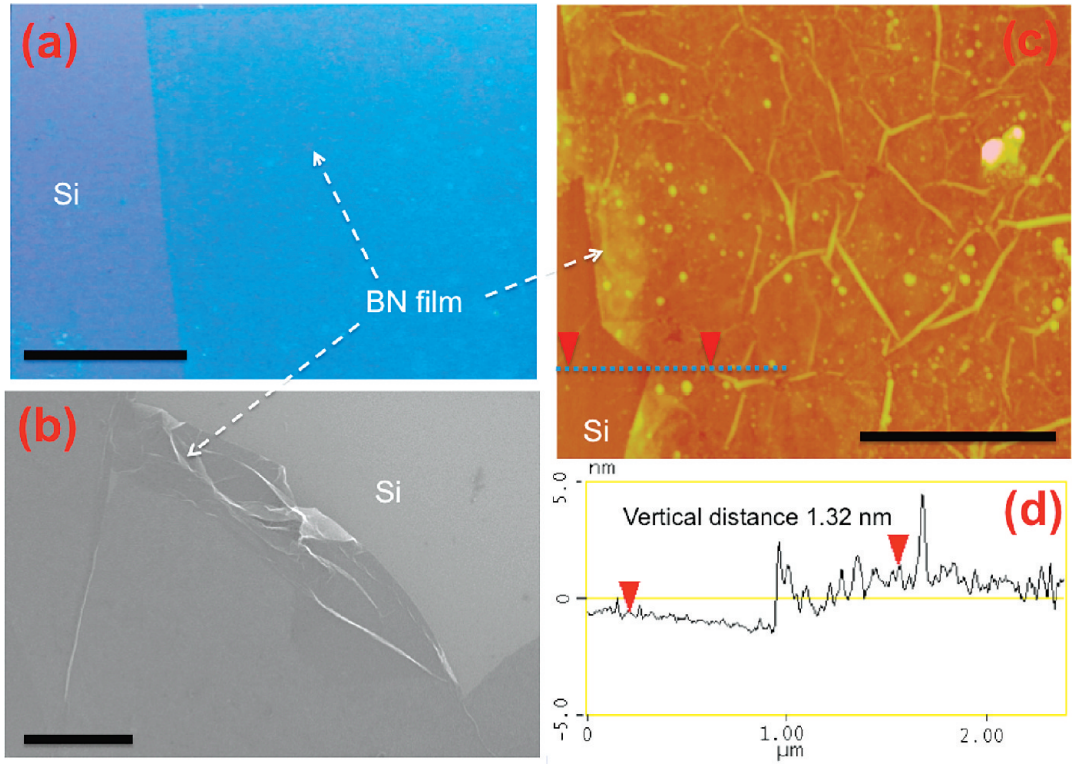

FIGURE 1. Topography of ultrathin hexagonal BN films. (a) Photograph of a large h-BN film on a silicon substrate. Scale bar is 1 cm. (b), SEM image shows a h-BN film (scale bar 10 μm). (c, d) AFM image and line-scan profile indicate that h-BN film has uniform thickness of a 1 nm. Scale bar is 2 μm.

copy (Agilent PicoScan 5500) was used to perform the following indention measurements.

Figure 1a is a photograph of as-grown h-BN film transferred onto a silicon substrate, showing that the grown films have continuous large areas up to several square centimeters. Panels b and c of Figure 1 show typical scanning electron microscopy (SEM) and atomic force microscopy (AFM) images of the film. Both optical imaging and electron microscopy images indicate that the film is quite uniform and continuous except for some wrinkles, which may be introduced by the transfer process and the roughness or gain boundaries present on the Cu surface.[14,17] Figure 1d shows the line-scan profile of films, indicating the as-grown films with thickness of about 1.3 nm.

HRTEM was performed to characterize the microstructure of these thin films. Our HRTEM observations found that the h-BN films mainly consist of two layers, as shown in Figure 2a. Some of the films were composed of three to five layers (Figure 2, panels b and c). To further evaluate the crystallinity of the films, SAED was carried out on the films. The SEAD of the region in Figure 2a is shown as the insert image, clearly revealing the distinctive hexagonal structure of h-BN films.[18] We mapped the elemental distribution of B and N in a selected area of the films by using energy-filtered techniques (see section 1 in Supporting Information). It is found that B and N are uniformly distributed over the entire area of the films. We performed atomic HRTEM characterization by using a low voltage aberration-corrected electron microscopy in order to investigate the atomic structure of the h-BN films. Figure 2d shows a typical atomic HRTEM image, in which the resolved features correspond to the hexagonal lattice having consistent lattice spacing with bulk h-BN.[19,20] The fast Fourier transform (FFT) analysis in Figure 2e reveals five sets of hexagonal spots, which indicates that the covered region of the Figure 2d has multiple layers. Using EELS, we qualitatively performed elemental analysis on the films to determine their chemical composition and structure. Figure 2f shows an EELS spectrum with two visible edges starting at around 180 and 390 eV, corresponding to the characteristic K-shell ionization edges of B and N, respectively.[19,21] The two bands corresponding to each element can be well resolved and show a first peak corresponding to the $1s-\pi^*$ antibonding orbit. This type of EELS edge structure proves that B and N are sp^2 hybridized[21,22] and indicates that the atomic films grown on Cu possess a hexagonal structure consisting of B and N, which is consistent with HRTEM observation.

The XPS spectra of as-grown h-BN films for the B and N edges are presented in panels a and b of Figure 3, respectively. It is previously reported that boron nitride bulk with hexagonal phase presents the B 1s core level at 190.1 eV.[23,24] We find that all our samples present a B 1s-core level at 189.9 eV (marked in Figure 3a), which is very close to that in h-BN bulk phase. The N 1s peak is located at 397.6 eV

DOI: 10.1021/nl1022139 | *Nano Lett.* **XXXX,** *xxx,* 000–000

NANO LETTERS

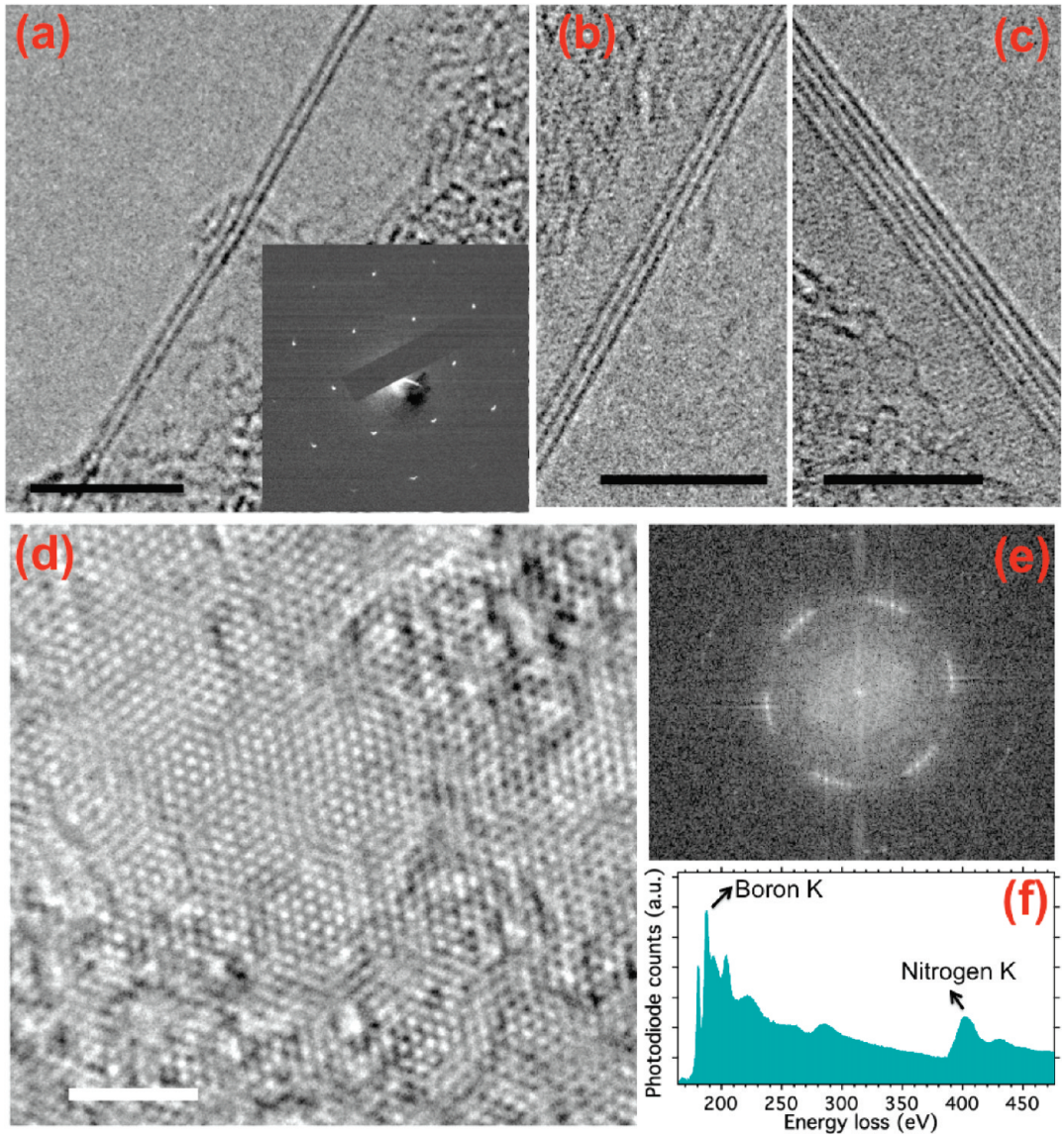

FIGURE 2. Microstructure of atomic layers hexagonal BN. (a) HRTEM images of the film edges indicate that the h-BN are two atomic layers thick. Some of as-grown films are three to five layers (b, c). The scale bar is 5 nm. The insert of (a) is the corresponding SEAD of the regions, which shows the hexagonal structure of h-BN film. (d) A typical atomic image of a h-BN films. The scale bars is 2 nm. (e) The FFT pattern of a region of panel d, which indicates a five-layer stacked region. (f) EELS spectrum of a h-BN film. The C signal corresponds to small amounts of amorphous carbon which could have come from contamination on TEM grids or contamination during transfer of the BN films.

(marked in Figure 3b), similarly to the reported position of the N1s spectrum (398.1 eV) of h-BN.[23,24] Both the B 1s and the N 1s spectra indicate that the configuration for B and N atoms is the B−N bond, implying that the hexagonal phase exists in our BN films. Figure 3c shows typical Raman spectra taken from the h-BN thin film (top curve) and a bulk h-BN (bottom curve). At the lower frequency region, the dominant peak near 1370 cm^{-1} that shows up intensely for both the film and the bulk samples is attributed to the B−N vibrational mode (E_{2g}) within h-BN layers.[25] This Raman spectrum further confirms the successful growth of BN film with a hexagonal structure. Figure 3d shows that the E_{2g} mode of h-BN film shifts to higher frequency compared with that for the bulk BN. The peak shift is about 2.5 cm^{-1}, and the fwhm decreases from 15.5 cm^{-1} in bulk BN to 11.7 cm^{-1} in the thin film. In general, a Raman peak frequency would shift to higher and lower frequency under compressive and tensile stress, respectively.[26] We speculate that the Raman peak frequency of the E_{2g} mode shifts to higher frequency due to an increase of stress in the h-BN films, which may be generated by the substrate interaction and the intrinsic surface wrinkles. At higher frequency region, the intensity of second mode for bulk BN gets suppressed due to a strong photoluminescence background, which is shown by a broad peak at 2765 cm^{-1}. The second-order Raman band of h-BN film is fitted by two peaks located at 2270 and 2631 cm^{-1}, as shown in the insert of Figure 3c.[27,28]

DOI: 10.1021/nl1022139 | *Nano Lett.* **XXXX,** *xxx,* 000–000

NANO LETTERS

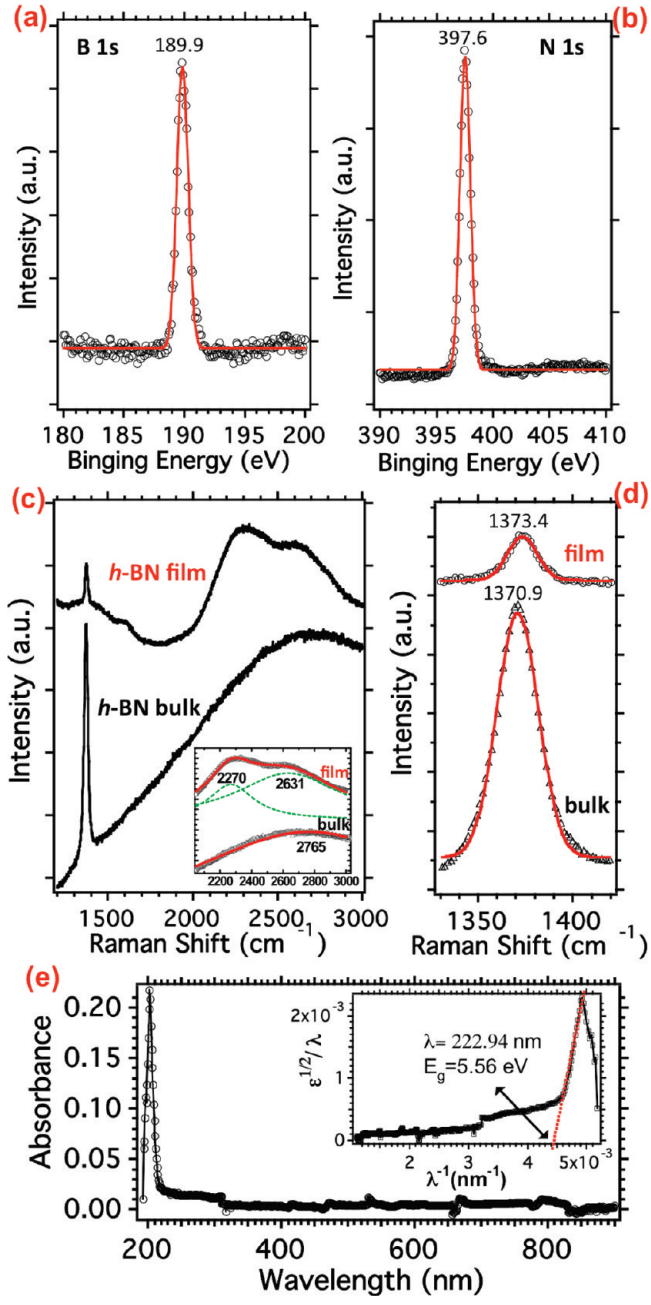

FIGURE 3. Spectra of hexagonal BN films. (a, b) XPS spectrum of B and N 1s core level, respectively. The spectral data (μ) are fitting by Gaussian curves (red solid). (c) Raman spectrum of a h-BN film and bulk *h*-BN recorded at room temperature, exited by 514.5 nm laser. The inset shows the peak at high frequency. (d) Their main Raman peak near 1370 cm^{-1}. The Lorenz curves (red solid) were used here to fit the peaks. (e) Ultraviolet−visible absorption spectra of h-BN films taken at room temperature. The inset shows the corresponding plot of $\varepsilon^{1/2}/\lambda$ versus $1/\lambda$.

Previous investigations have shown that bulk hexagonal BN is a wide gap material. Here, we performed electrical measurements on h-BN films devices, fabricated by standard lithography technique (see section 2 in Supporting Information). We found that the h-BN films are very good insulators. The UV−visible absorption spectrum was carried out for investigating the optical energy gap of the h-BN film based on its optically induced transition. For this study, we first transferred large h-BN film onto an optical quartz plate, and the quartz background was subtracted using a blank quartz plate as the reference substrate. The following Tauc's equation was used to determine the optical band gap E_g[29]

$$\omega^2\varepsilon = (h\omega - E_g)^2 \quad (1)$$

where ε is the optical absorbance and $\omega = 2\pi/\lambda$ is the angular frequency of the incident radiation (λ is the wavelength). As Figure 3e shows, the nanometer thick h-BN film is highly transparent and can transmit over 99% of the light with wavelengths in the range of 250−900 nm. The absorption spectrum displays one sharp absorption peak at 203 nm. On the basis of Tauc's formulation, it is speculated that the plot of $\varepsilon^{1/2}/\lambda$ versus $1/\lambda$ should be a straight line at the absorption range. Therefore, the intersection point with the x axis is $1/\lambda_g$ (λ_g is defined as the gap wavelength). The optical band gap can be calculated based on $E_g = hc/\lambda_g$. The insert plot of Figure 3e shows $\varepsilon^{1/2}/\lambda$ versus $1/\lambda$ curve acquired from the thin h-BN film. The calculated gap wavelength λ_g is about 223 nm, which corresponds to an optical band gap of 5.56 eV. Previous theoretical calculations of band structures for a single layer of h-BN anticipated that equivalent bands did not cross each other and a 6 eV band gap was the result.[30] Considering two to five layers in our h-BN films, the measured gap is smaller than the theoretical gap value of a single layer due to the layer−layer interaction increases the dispersion of the electronic bands and tends to reduce the gap,[30] but it is larger than that of bulk h-BN (5.2−5.4 eV).[30,31]

Theoretical calculations have indicated that BN layers can be extremely strong.[32] To investigate mechanical properties of the h-BN films, circular wells with diameter around 1 μm were patterned onto a silicon substrate by e-beam lithography and reactive ion etching (RIE) techniques. The h-BN films were then transferred onto the prepatterned substrates. Figure 4a shows an ultrathin film deposited over many circular wells to form a series of freestanding membranes. Noncontact mode AFM test was first used to obtain the thickness and find the center of the suspended near circular membranes. It is found that the h-BN films were stretched tautly across the well openings with about 20−50 nm sag due to the van der Waals attraction from the substrate and surface tension during drying process (Figure S3b in Supporting Information). The mechanical properties of the h-BN films were probed by indenting the center of each freestanding membrane with a diamond tip, as illustrated in Figure 4b. The detail indention test can be found in section 3 of Supporting Information. The elastic response of a 2D film

DOI: 10.1021/nl1022139 | *Nano Lett.* **XXXX,** *xxx,* 000−000

NANO LETTERS

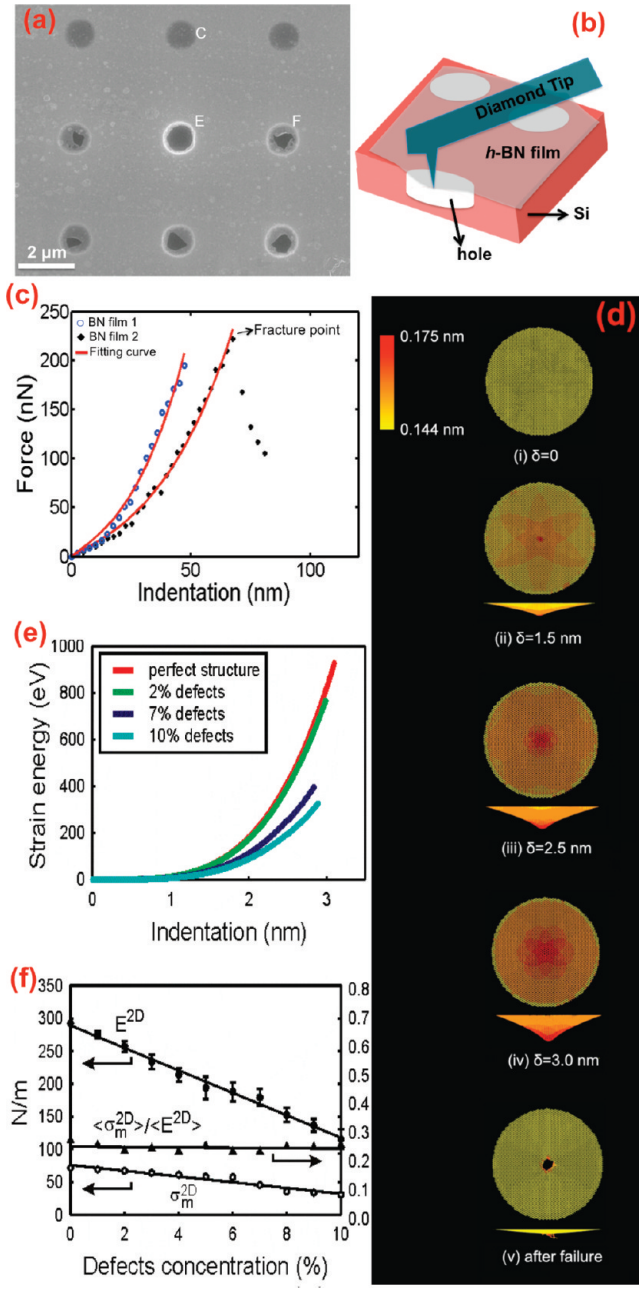

FIGURE 4. Elastic properties and intrinsic strength of ultrathin hexagonal BN film. (a) Scanning electron micrograph of a large h-BN film spanning an array of circular holes 1 μm in diameter. Area C shows a hole fully covered by h-BN, and area F is fractured from indentation. (b) Schematic of nanoindentation on suspended h-BN membrane. (c) Measured force vs displacement curve and fracture loading curve for two 1.1 μm diameter membranes and curves fitting to eq 2. The fracture point was marked. (d) The deformation sequence for of BN membrane: (i) unloaded structure, (ii−iv) with indentation depth δ = 1.5 nm, 2.5 nm, 3.0 nm (critical stain), and (v) after the failure. The color variations represent the bond lengths, from red (0.161−0.175 nm) to yellow (0.144−0.146 nm). (e) The strain energy of the BN sheet as a function of the indentation depth, for different vacancy concentrations. (f) The dependence of modulus E^{2D}, breaking stress $\sigma_m{}^{2D}$, and breaking strain ε on the vacancy concentration.

is expected to be nonlinear, and the value of mechanical properties was determined by the equations[33]

$$F = \sigma^{2D}(\pi a)(\delta/a) + E^{2D}(q^3 a)(\delta/a)^3 \quad (2)$$

where F is applied force, σ^{2D} is the pretension in the film, a is the radius of wells, and E^{2D} is the elastic constant. δ is the deflection at the center point; $q = 0.99$ is a dimensionless constant related to the Poisson's ratio of boron nitride.[34] Figure 4c shows two typical force−displacement curves (open circles) recorded on two h-BN films stretched tautly across 1.1 μm wells. The data are fitted by polynomial curves according to eq 2, taking σ^{2D} and E^{2D} as free parameters. The calculated values of E^{2D} for the h-BN film with thickness of 1−2 nm are in the range of 220−510 N·m^{-1}. Considering the two films stacked with two and five hexagonal BN layers, the tested 2D modulus of h-BN in our case is lower than the theoretical computation (270 N·m^{-1} for single BN layer).[33,34] It may be attributed to the layer distribution of stacking faults in the CVD grown films[35] or the error in estimating the exact diameter of the holes and the position of membrane contact with the substrate. The breaking strength of h-BN films was measured by loading the membranes to the breaking point. The image in Figure 4a ("F" region) shows the fractured membranes after being broken by a diamond tip, also indicating that the indentation tests were performed at the center of free-standing h-BN membrane. A typical fracture test curve is presented in Figure 4c. It can see that the films break at deflections of about 70 nm and forces of about 221 nN. A continuum model was used to determine the maximum stress of a clamped circular membrane[33]

$$\sigma_m{}^{2D} = (FE^{2D}/4\pi R)^{1/2} \quad (3)$$

where $\sigma_m{}^{2D}$ is the maximum stress at the central point of the film and $R = 50$ nm is the radius of our indenter tip. The calculated breaking strength is about 8.8 N·m^{-1} for our ultrathin h-BN film with a thickness of around 1 nm. We note that the strain here was much smaller than that of graphene reported in ref 33, and hence we ignored the nonlinearity effect and used a linear model in eq 3. We suggest that the lower breaking stress in the h-BN film compared with monolayer graphene could be due to possible vacancy defects in our freestanding as-grown membranes.[33,35] Somewhat reduced stiffness of the h-BN layers can be either caused by compliance at the edges (hole perimeter) or due to the presence of defects. We illustrate the latter with molecular mechanics simulations. Figure 4d shows the simulation process of the deformation of h-BN membrane, including the initial, strained, and fractured structure. The pressure induced by the tip causes the greatest BN-bond elongation in the vicinity of the tip, as indicated by the color gradient (Figure 4d, ii−iv). To

DOI: 10.1021/nl1022139 | Nano Lett. XXXX, xxx, 000–000

NANO LETTERS

TABLE 1. The Comparison of Mechanical Properties of h-BN Films with Different Thicknesses and Theoretical Computation Values

sample	thickness (nm)	possible layer no.	E^{2D} (N/m)	$\sigma_m{}^{2D}$ (N/m)
A	2.0 ± 0.1	~5	503 ± 30	15.7 ± 1.5
B	1.65 ± 0.1	~4	431 ± 21	12.8 ± 1.3
C	1.03 ± 0.1	~2	223 ± 16	8.8 ± 1.2
theoreticalcomputation	0.33	1	292.1	71.7

emulate the AFM tip, a hemisphere of mutually static atoms strain the h-BN membrane with fixed edges up to its failure. At critical strain level, the film fails with a visible puncture in the center. The computed strain energy (Figure 4e) is then fitted to the integral of eq 2, to obtain the coefficient E^{2D}.

For the computation model, we chose a BN sheet of diameter 14.8 nm and a tip of diameter 1.63 nm. Then for an initially perfect BN sheet, we obtain $E^{2D} = 292.1\ N \cdot m^{-1}$, in accordance with earlier ab initio results (271 N/m).[34] We simulated the behavior of BN sheets with 1−10% vacancy concentrations. Due to variability in defect distributions, we performed 10 computational tests for each of the concentration values and plotted the obtained data in Figure 4e. The E^{2D} values decrease almost linearly with defect concentration, down to 115.4 ± 14.8 N/m (at 10% vacancies). The $\sigma_m{}^{2D}$ decreases linearly from 71.7 N/m (perfect BN) to 26.6 ± 1.7 N/m (10% vacancies). It is important to note that the breaking strain $e = \langle\sigma_m{}^{2D}\rangle/\langle E^{2D}\rangle \approx 0.22$ is nearly unaffected by vacancies. This contrasts with the well-known stress-concentration by microcracks but is understandable for atomic-size voids. A comparison between tested mechanical values and theoretical computations is listed in Table 1. More information of computeration is shown in section 4 of the Supporting Information. Here, we want to point out that the tested values may have been underestimated due to the nonsharp edges of the wells and the possible underestimation of the diameter of freestanding BN membranes. Possible defect distribution in the films could also contribute to the relatively lower values in our tip-indentation experiments.

As to the growth mechanism of hexagonal boron nitride, it has been observed that small area h-BN layers, such as BN nanomeshes and islands, could be synthesized by decomposed borazine $(HBNH)_3$ or B-trichloroborazine $(ClBNH)_3$ on transition metal surfaces using a CVD process at 1000−1100 K.[12,36] In our synthesis, the copper substrate has a lattice constant similar to that of the in-plane lattice constant of *h*-BN (0.255 nm versus 0.25 nm). The copper substrate shows catalytic activity for the decomposition of ammonia borane (NH_3−BH_3). During growth, the ammonia borane was sublimed first and transferred to a high temperature zone for decomposition. The decomposition of NH_3−BH_3 vapor at 1300 K on a copper surface supplies both boron and nitrogen onto the metallic substrate, leading to surface diffusion of these species and a surface-mediated growth of h-BN films, which is similar to the growth mechanism proposed for graphene and BN-C hybrid layers on copper.[14,16,37] As the growth seems to occur by a surface-mediated process, the quality of copper foil plays a key role in controlling the formation of continuous layers on the substrate and the number of layers of h-BN formed. It is not clear however why the growth produces mostly multiple layers of h-BN and not a single layer; with further optimization of growth parameters, this could be achieved in the future but for applications involving the use of h-BN layers as dielectric, a few layer structure may suffice.

In summary, we have synthesized two-dimensional atomic layers of hexagonal BN films over large areas and transferred them successfully to many substrates. These 2D dielectric films with a large optical band gap of 5.56 eV show high optical transparency in the UV−visible range. The mechanical properties of the h-BN film were measured via nanoindentation and theoretical models and this showed the dependence of the in-plane stiffness of the films to intrinsic defects present in the films. Our synthesis method could pave a way for investigating the unique structure and properties of h-BN thin films[38] and exploiting its large number of potential applications[39,40] including its use as a dielectric to complement graphene devices.

Acknowledgment. P.M.A. acknowledge support from Rice University startup funds and funding support from the Office of Naval Research (ONR) through the MURI program on graphene and the Basic Energy Sciences division of the Department of Energy (DOE). L.S. was supported by DOE-BES program DE-SC0001479 for the growth and characterization. L.C. was supported by the ONR MURI program (Award No N00014-09-1-1066) for TEM characterization. C.J. acknowledges the International Balzan Foundation for financial support through Meijo University. J.N. acknowledges the scholarship from Chinese State Scholarship fund. H.L. and J.L. acknowledge support from NSF (ECCS-0702766) and the Welch Foundation (C-1716). P.S. and B.Y. acknowledge support from a DOE grant (DE-FG02-09ER46598).

Supporting Information Available. Elemental mapping by transmission electron microscopy on the h-BN film, electrical measurement on the h-BN film, detail of the indentation measurements by atomic force microscopy, and molecular mechanics computation of h-BN layer.This material is available free of charge via the Internet at http://pubs.acs.org.

REFERENCES AND NOTES

(1) Watanabe, K.; Taniguchi, T.; Kanda, H. Direct-bandgap properties and evidence for ultraviolet lasing of hexagonal boron nitride single crystal. *Nat. Mater.* **2004**, *3*, 404–409.
(2) Kubota, Y.; Watanabe, K.; Tsuda, O.; Taniguchi, T. Deep ultraviolet light-emitting hexagonal boron nitride synthesized at atmospheric pressure. *Science* **2007**, *317*, 932–934.
(3) Golberg, D.; Bando, Y.; Huang, Y.; Terao, T.; Mitome, M.; Tang, C.; Zhi, C. Boron nitride nanotubes and nanotsheets. *ACS Nano* **2010**, *4*, 2979–2993.
(4) Pacile, D.; Meyer, J. C.; Girit, C. O.; Zettl, A. The two-dimensional phase of boron nitride: few-atomic-layer sheets and suspended membranes. *Appl. Phys. Lett.* **2008**, *92*, 133107–1.

DOI: 10.1021/nl1022139 | *Nano Lett.* **XXXX,** *xxx,* 000–000

NANO LETTERS

(5) Lee, C. G.; Li, Q.; Kalb, W.; Liu, X.; Berger, H.; Carpick, R. W.; Hone, J. Frictional characteristics of atomically thin sheets. *Science* **2010**, *328*, 76–80.

(6) Dean, C. R.; Young, A. F.; Meric, I.; Lee, C.; Wang, L.; Sorgenfrei, S.; Watanabe, K.; Taniguchi, T., Kim, P.; Shepard, K. L.; Hone, J. Boron nitride substrates for high quality graphene electronics. arXiv: 1005.4917, 2010.

(7) Giovannetti, G.; Khomyakov, P.; Brocks, G.; Kelly, P.; Brink, J. V. D. Substrate-induced band gap in graphene on hexagonal boron nitride: Ab initio density functional calculations. *Phys. Rev. B* **2007**, *76*, No. 073103.

(8) Zhi, C.; Bando, Y.; Tang, C.; Kuwahara, H.; Golberg, D. Large-scale fabrication of boron nitride nanosheets and their utilization in polymeric composites with improved thermal and mechanical properties. *Adv. Mater.* **2009**, *21*, 2889–2893.

(9) Mayer, J. C.; Chuvilin, A.; Algara-Siller, G.; Biskupek, J.; Kaiser, U. Selective sputtering and atomic resolution imaging of atomically thin boron nitride membranes. *Nano Lett.* **2009**, *9*, 2683–2689.

(10) Nag, A.; Raidongia, K.; Hembram, K. P. S. S.; Datta, R.; Waghmare, U. V.; Rao, C. N. R. Graphene analogues of BN: novel synthesis and properties. *ACS Nano* **2010**, *4*, 1539–1544.

(11) Nagashima, A.; Tejima, N.; Gamou, Y.; Kawai, T.; Oshima, C. Electronic structure of monolayer hexagonal boron nitride physisorbed on metal surfaces. *Phys. Rev. Lett.* **1995**, *75*, 3918–3921.

(12) Corso, M.; Auwarter, W.; Muntwiler, M.; Tamai, A.; Greber, T.; Osterwalder, J. Boron nitride nanomesh. *Science* **2004**, *303*, 217–220.

(13) Auwarter, W.; Suter, H. U.; Sachdev, H.; Greber, T. Synthesis of one monolayer of hexagonal boron nitride on Ni(111) from B-Trichloroborazine ($ClBNH)_3$. *Chem. Mater.* **2004**, *16*, 343–345.

(14) Li, X.; Cai, W.; An, J.; Kim, S.; Nah, J.; Yang, D.; Piner, R.; Velamakanni, A.; Jung, I.; Tutuc, E.; Banerjee, S. K.; Colombo, L.; Ruoff, R. S. Large-area synthesis of high-quality and uniform graphene films on copper foils. *Science* **2009**, *324*, 1312–1314.

(15) Preobrajenski, A. B.; Vinogradov, A. S.; Mårtensson, N. Monolayer of *h*-BN chemisorbed on Cu(111) and Ni(111). *Surf. Sci.* **2005**, *582*, 21–30.

(16) Ci, L.; Song, L.; Jin, C.; Jariwala, D.; Wu, D.; Li, Y.; Srivastava, A.; Wang, Z. F.; Storr, K.; Balicas, L.; Liu, F.; Ajayan, P. M. Atomic layers of hybridized boron nitride and graphene domains. *Nat. Mater.* **2010**, *9*, 430–435.

(17) Li, X.; Zhu, Y.; Cai, W.; Borysiak, M.; Han, B.; Chen, D.; Piner, R. D.; Colombo, L.; Ruoff, R. S. Transfer of large-area graphene films for high-performance transparent conductive electrodes. *Nano Lett.* **2009**, *9*, 4359–4363.

(18) Regan, W.; Alem, N.; Aleman, B.; Geng, B.; Girit, C.; Maserati, L.; Wang, F.; Crommie, M.; Zettl, A. A direct transfer of layer-area graphene. *Appl. Phys. Lett.* **2010**, *96*, 113102.

(19) Jin, C.; Lin, F.; Suenaga, K.; Iijima, S. Fabrication of a freestanding boron nitride single layer and its defect assignments. *Phys. Rev. Lett.* **2009**, *102*, 195505.

(20) Alem, N.; Emi, R.; Kisielowski, C.; Rossell, M. D.; Gannett, W.; Zettl, A. Atomically thin hexagonal boron nitride probe by ultra-high-resolution transmission electron microscopy. *Phys. Rev. B* **2009**, *80*, 155425–1.

(21) Chopra, N. G.; Luyken, R. J.; Cherrey, K.; Crespi, V. H.; Cohen, M. L.; Louie, S. G.; Zettl, A. Boron nitride nanotubes. *Science* **1995**, *269*, 966–967.

(22) Wibbelt, M.; Kohl, H.; Kohler-Redlich, Ph. Multiple-scattering calculations of electron-energy-loss near-edge structrues of existing and predicted phases in the ternary system B-C-N. *Phys. Rev. B* **1999**, *59*, 11739–11745.

(23) Moulder, J. F.; Stickle, W. F.; Sobol, P. E.; Bombem, D. *Handbook of X-ray Photoeletron spectroscopy*; Chastain, J., Ed.; Perkin Elmer Co.: Eden Prairie, MN, 1992.

(24) Park, K. S.; Lee, D. Y.; Kim, K. J.; Moon, D. W. Observation of a hexagonal BN surface layer on the cubic BN film grown by dual ion beam sputter deposition. *Appl. Phys. Lett.* **1997**, *70*, 315–317.

(25) Geick, R.; Perry, C. H.; Rupprecht, G. Normal modes in hexagonal boron nitride. *Phys. Rev.* **1966**, *146*, 543–547.

(26) Kuzuba, T.; Sato, Y.; Yamaoka, S.; Era, K. Raman-scattering study of high-pressure effects on the anisotropy of force constants of hexagonal boron nitride. *Phys. Rev. B* **1978**, *18*, 4440–4443.

(27) Wu, J.; Han, W.; Walukiewicz, W.; Ager, J. W., III; Shan, W.; Haller, E. E.; Zettl, A. Raman spectroscopy and time-resolved photoluminescence of BN and BCN nanotubes. *Nano Lett.* **2004**, *4*, 647–650.

(28) Ferrari, A. C.; Meyer, J. C.; Scardaci, V.; Casiraghi, C.; Lazzeri, M.; Mauri, F.; Piscanec, S.; Jiang, D.; Novoselov, K. S.; Roth, S.; Geim, A. K. Raman spectrum of graphene and graphene layers. *Phys. Rev. Lett.* **2006**, *97*, 187401.

(29) Tauc, J.; Grigorovici, R.; Vancu, A. Optical properties and electronic structure of amorphous germanium. *Phys. Status Solidi* **1996**, *15*, 627–637.

(30) Blase, X.; Rubio, A.; Louie, S. G.; Cohen, M. L. Quasiparticle band structure of bulk hexagonal boron nitride and related systems. *Phys. Rev. B* **1995**, *51*, 6868–6875.

(31) Zunger, A.; Katzir, A.; Halperin, A. Optical properties of hexagonal boron nitride. *Phys. Rev. B* **1976**, *13*, 5560–5573.

(32) Hemandez, E.; Goze, C.; Bernier, P.; Rubio, A. Elastic properties of C and BCN composite nanotubes. *Phys. Rev. Lett.* **1998**, *68*, 4502–4505.

(33) Lee, C.; Wei, X.; Kysar, W. J.; Hone, J. Measurement of the elastic properties and intrisic strength of monolayer graphene. *Science* **2008**, *321*, 385–388.

(34) Kudin, K. N.; Scuseria, G. E.; Yakobson, B. I. C_2F, BN, and C nanoshell elasticity from ab inition computations. *Phys. Rev. B* **2001**, *64*, 235406.

(35) Li, C.; Bando, Y.; Zhi, C.; Huang, Y.; Golberg, D. Thickness-dependent bending modulus of hexagonal boron nitride nanosheets. *Nanotechnology* **2009**, *20*, 385707.

(36) Auwarter, W.; Suter, H. U.; Sachdev, H.; Greber, T. Synthesis of one monolayer of hexagonal boron nitride on Ni(111) from B-Trichloroborazine. *Chem. Mater.* **2004**, *16*, 343–345.

(37) Li, X.; Cai, W.; Colombo, L.; Ruoff, R. S. Evolution of graphene growth on Ni and Cu by carbon isotope labeling. *Nano Lett.* **2009**, *9*, 4268–4272.

(38) Stephan, O.; Ajayan, P. M.; Colliex, C.; Redlich, Ph.; Lambert, J. M.; Bernier, P.; Lefin, P. Doping graphitic and carbon nanotube structures with boron and nitrogen. *Science* **1994**, *266*, 1683–1685.

(39) Davis, R. F. III−V Nitrides for electronic and optoelectronic applications. *Proc. IEEE* **1991**, *79*, 702–712.

(40) Engler, M.; Lesniak, C.; Ruisinger, B.; Eichler, J. Hexagonal boron nitride (hBN)-applications from metallurgy to cosmetics. *Cfi/Ber. DKG* **2007**, *84*, E49–E53.

DOI: 10.1021/nl1022139 | *Nano Lett.* **XXXX,** *xxx,* 000–000